



Original article

Spermiogenesis in the African sideneck turtle (*Pelusios castaneus*): Acrosomal vesicle formation and nuclear morphogenesisSamuel G. Olukole^{a,b,*}, Mary-Catherine Madekurozwa^a, Bankole O. Oke^b^a Department of Anatomy and Physiology, Faculty of Veterinary Science, University of Pretoria, South Africa^b Department of Veterinary Anatomy, Faculty of Veterinary Medicine, University of Ibadan, Ibadan, Nigeria

ARTICLE INFO

Article history:

Received 1 December 2016

Accepted 23 February 2017

Available online 27 February 2017

Keywords:

Acrosomal vesicle

Spermatid

Spermiogenesis

Turtle

Ultrastructure

ABSTRACT

Testicular samples were collected from African sideneck turtles (*Pelusios castaneus*) at the peak of spermiogenesis in order to describe spermatid acrosomal vesicle formation and nuclear morphogenesis. Acrosomal vesicle formation commences with a Golgi transport vesicle attaching to a round spermatid, followed by the emergence of an acrosome granule. This is followed by the development of the sub-acrosomal space, which becomes enlarged as nuclear elongation and condensation continue. The round spermatid elongates and the emerging elongating spermatid successively becomes surrounded by circular, longitudinal and slanting microtubules of the manchette. The acrosomal vesicle becomes visible with an acrosome granule resting on the base of the electron dense material. Acrosomal vesicle morphogenesis in the African sideneck turtle results in a highly compartmentalized acrosome divisible into the acrosomal cortex and medulla. The future position of the flagellum starts to develop, being encircled by mitochondria while the distal centriole becomes obvious and the emerging flagellum grossly divisible into the connecting piece, midpiece, principal piece and endpiece. Although acrosomal vesicle formation and nuclear morphogenesis during spermiogenesis in the turtle are consistent with other reptilian species, a few differences were observed. The major difference observed was the formation of a single acrosome granule, which manifests prior to the attachment of the acrosomal vesicle to spermatid nucleus. The other differences observed were the emergence of two endonuclear canals in the elongating spermatid and the presence of slanting microtubules of the manchette. The observed developmental variations are expected to be valuable in future phylogenetic studies and potentially serve to test certain hypotheses concerning the reproductive status of turtle species. Findings from this study add to the growing database of spermatid morphology in turtles, thereby providing insights into variations in mature sperm morphology in the species.

© 2017 The Authors. Production and hosting by Elsevier B.V. on behalf of King Saud University. This is an open access article under the CC BY-NC-ND license (<http://creativecommons.org/licenses/by-nc-nd/4.0/>).

1. Introduction

The African sideneck turtle (*Pelusios castaneus*) is a freshwater turtle widely distributed in West Africa (Kirkpatrick, 1995). The turtle is small to medium in size, with a relatively extensive plas-

tron that may have a hinge present between the pectoral and abdominal scutes (Olukole et al., 2010).

Studies on the ultrastructure of spermatozoa of reptiles have provided knowledge on the development and functional significance of many spermatozoal organelles (Teixeira et al., 1999; Al-Dokhi, 2004; Al-Dokhi et al., 2007, 2015) while elucidating the relationship between these components and reproductive activities (Gribbins, 2011). Similar to the mammalian, the reptilian spermatozoon consists of a head region containing the nucleus and the acrosomal structures, a midpiece, and a tail region which is subdivided into principal and end-pieces (Teixeira et al., 1999; Al-Dokhi and Al-Wasel, 2001a).

Extensive ultrastructural studies on spermiogenesis in reptiles have been conducted within the last decade. This include Jamaican gray anole, *Anolis lineatropus* (Rheubert et al., 2010a); black swamp snake, *Seminatrix pygaea* (Rheubert et al., 2010b); lizard *Iguana*

* Corresponding author at: Department of Veterinary Anatomy, Faculty of Veterinary Medicine, University of Ibadan, Ibadan, Nigeria.

E-mail addresses: Debo.Olukole@up.ac.za, deborolukole@yahoo.com, sg.olukole@mail.ui.edu.ng (S.G. Olukole).

Peer review under responsibility of King Saud University.



Production and hosting by Elsevier

iguana (Vieira et al., 2004, 2005, 2007); American alligator, *Alligator mississippiensis* (Gribbins et al., 2010) and Mediterranean gecko, *Hemidactylus turcicus* (Rheubert et al., 2011).

Ultrastructural studies on spermiogenesis in turtles have been carried out on the freshwater turtle, *Maurymes caspica* (Al-Dokhi and Al-Wasel, 2001a,b) as well as the soft shell turtles- *Trionyx sinensis* (Chen et al., 2006) and *Pelodiscus sinensis* (Zhang et al., 2007). Nevertheless, there is a scarcity of information on the ultrastructure of spermiogenesis in freshwater turtles of African origin. At present, spermatogenesis in the African sideneck turtle has only been studied at the light microscope level (Olukole et al., 2013, 2014). The current study, being the first of this nature performed in a turtle species of African origin, aims to describe acrosomal vesicle formation and nuclear morphogenesis during spermiogenesis in the African sideneck with the view of generating data useful in the reproductive biology of the turtle.

2. Materials and methods

2.1. Experimental animals

Ten adult male African sideneck turtles (*Pelusios castaneus*) with an average bodyweight of 0.72 kg and average curved carapace length of 26.4 ± 1.87 cm, were sampled in August and September, a period of peak spermiogenesis (Olukole et al., 2014). The ten turtles were parts of sixty turtles sampled on the basis of five turtles per month for a calendar year during the process of investigating the annual spermiogenic cycle in the turtles (Olukole et al., 2014). The turtles were collected from river drainages in Ibadan (Ogunpa, Odo-Ona, Odo-Oba and Oke-Ayo), Nigeria. Carapacial and plastral characteristics of the turtle, as described by Kirkpatrick (1995), were used in the determination of adulthood in the turtles. The turtles were anaesthetized with an intramuscular injection of ketamine-HCl (25 mg/kg body-weight). The animals were subsequently sacrificed by cervical decapitation. The testes were removed after separating the plastron from the carapace. All procedures were carried out according to the guidelines for the care and use of experimental animals (National Institute of Health (NIH), USA. The study was approved by the University of Ibadan Animal Care and Use Research Ethics Committee (UIA-CUREC: 12/13/05).

2.1.1. Light microscopy

Samples of the testes were fixed in Bouin's fluid and embedded in paraffin blocks. Sections 2–4 μ m thick were stained with Haematoxylin and Eosin, as well as the Periodic Acid Schiff (PAS) (Rao and Shaad, 1985). The slides were then studied under a light microscope (Olympus BX63 with a DP72 camera).

2.2. Transmission electron microscopy

Additional testicular tissues were fixed in glutaraldehyde in 0.1 M sodium cacodylate buffer (pH 7.2) for 4 h at 4 °C. The samples were then thoroughly washed in the same buffer, post-fixed in 1% osmium tetroxide, and subsequently dehydrated in a graded series of ethanol solutions. Tissues were then cleared with propylene oxide, infiltrated with a 1:1 solution of propylene oxide: epoxy resin, 1:2 solution of propylene oxide:epoxy resin, and then placed in 100% epoxy resin for 36 h under vacuum. The samples were embedded in fresh epoxy resin and cured at 60 °C for 48 h. Semi-thin sections were stained with toluidine blue and observed under the light microscope (Olympus BX63 with a DP72 camera). Ultra-thin sections (70–80 nm) were cut with a diamond knife on an ultramicrotome (Ultracut- Reichert, Austria). The sections were

then double stained with uranyl acetate and lead acetate. The copper grids were examined under a transmission electron microscope (Philips CM 10 TEM) operating at 80 kv. Representative micrographs of different stages of spermiogenesis were taken

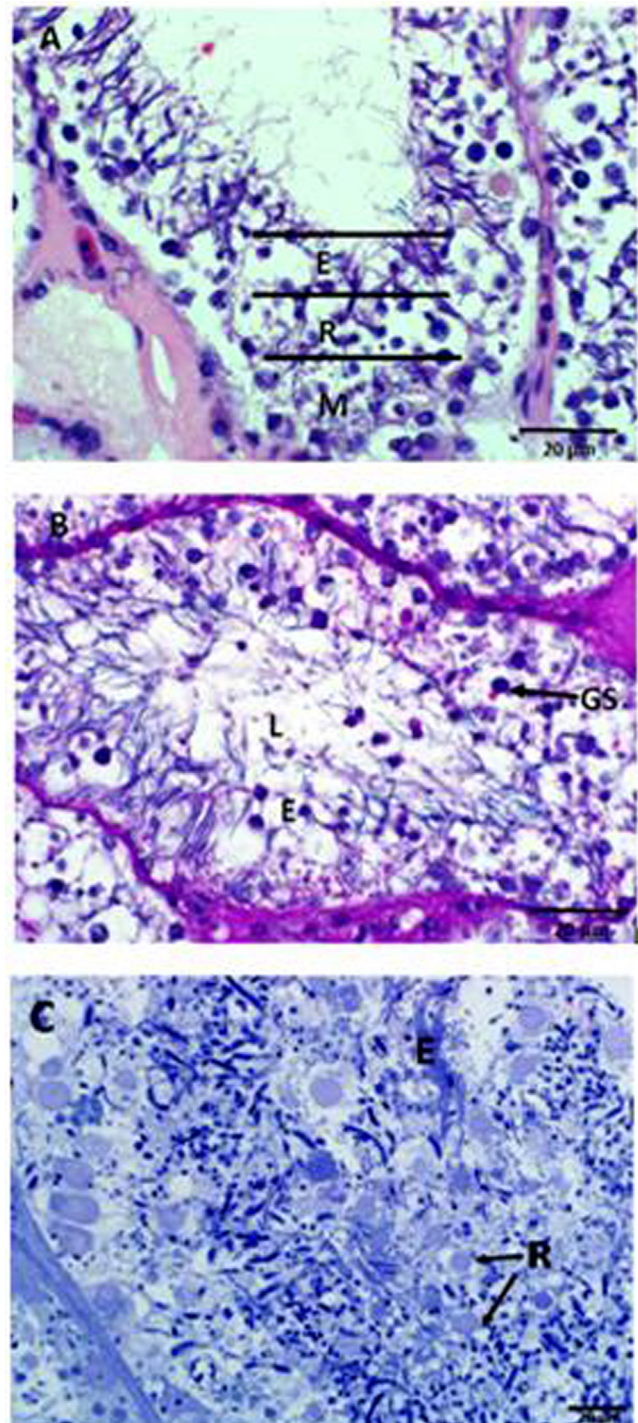


Fig. 1. Light microscope photomicrograph of the seminiferous epithelium in the African sideneck turtle. A. Regional distribution of cells within the seminiferous tubule, M: region of spermatogonia and spermatocytes; R: region of round spermatids; E: region of elongating spermatids; L: lumen, where spermatozoa will be released after the completion of spermiogenesis (H&E). B. PAS-positive Golgi vesicles (GS), elongating spermatids (E) and the lumen (L) of the seminiferous tubule (PAS). C. Toluidine-blue-positive round spermatids (R) and elongating spermatids (E) towards the adluminal compartment of the seminiferous tubule (Toluidine-Blue).

using a Gatan 785 Erlangshen digital camera (GatanInc., Warrendale, PA). Analysis and assembling of composite micrographs were carried out using Adobe Photoshop CS5 (Adobe Systems, San Jose, CA).

3. Results

The distribution of germ cells from the basement membrane of the seminiferous tubule to its luminal compartment is comprised of spermatogonia, spermatocytes, round spermatids, elongating spermatids and spermatozoa (Fig. 1A). Upon the completion of the second meiotic division, secondary spermatocytes develop into round spermatids, which accumulate in the adluminal compartment of the seminiferous epithelium thereby marking the onset of spermiogenesis in the African sideneck turtle (Fig. 1A). At this stage, the cytoplasm of round (early) spermatids, displays Golgi vesicles, which are PAS and toluidine blue-positive (Fig. 1B & C). Toluidine blue-positive round spermatids, as well as elongating spermatids are observed towards the adluminal compartments of the seminiferous tubules (Fig. 1C).

Ultrastructurally, round spermatids exhibit a prominent juxtanuclear Golgi complex consisting of flattened cisternae and vesicles of different sizes, which originate from the complex (Fig. 2A). At this stage, the early round spermatid shows heterogeneous nuclear chromatin and cytoplasm which contains prominent ovoid or elliptical mitochondria. The first major observable morphological change in the state of the round spermatid is the

hypertrophy of the Golgi complex, followed by an increase in the number and size of the detaching vesicles. At this stage, microvesicles and several mitochondria surround the nucleus of the spermatid (Fig. 2B). These small vesicles coalesce, giving rise to the formation of a large voluminous vesicle, the macrovesicle (Fig. 2C). The macrovesicle, which is also known as the proacrosomal vesicle, attaches to the nuclear membrane of the spermatid forming an electron dense layer at its point of attachment (Fig. 2C). This stage is followed by the gradual flattening of the proacrosomal vesicle, thereby forming the acrosomal vesicle (Fig. 2D).

Towards the end of the round spermatid stage, the most distal part of the nucleus starts to elongate and nuclear chromatin begins to condense (Fig. 3A). As differentiation continues, an acrosomal granule, positioned at the base of electron dense material, develops (Fig. 3B). At this stage the acrosome vesicle has spread to cover the proximal part of the spermatid nucleus and two parallel intranuclear tubules have formed in the interior of the nucleus (Fig. 3B). The formation of the acrosome vesicle is then complete and the spermatid is set for nuclear elongation and condensation. As nuclear elongation and condensation commence, during the early stage of spermatid elongation, centrally-placed nuclear chromatin becomes prominent. This is concomitant with the proximal streamlining of the acrosomal vesicle (Fig. 3C). The cytoplasm of the spermatid begins to shift causing mitochondria and rough endoplasmic reticular cisternae to relocate to the basal portions of the cell. As nuclear elongation and condensation progress, the

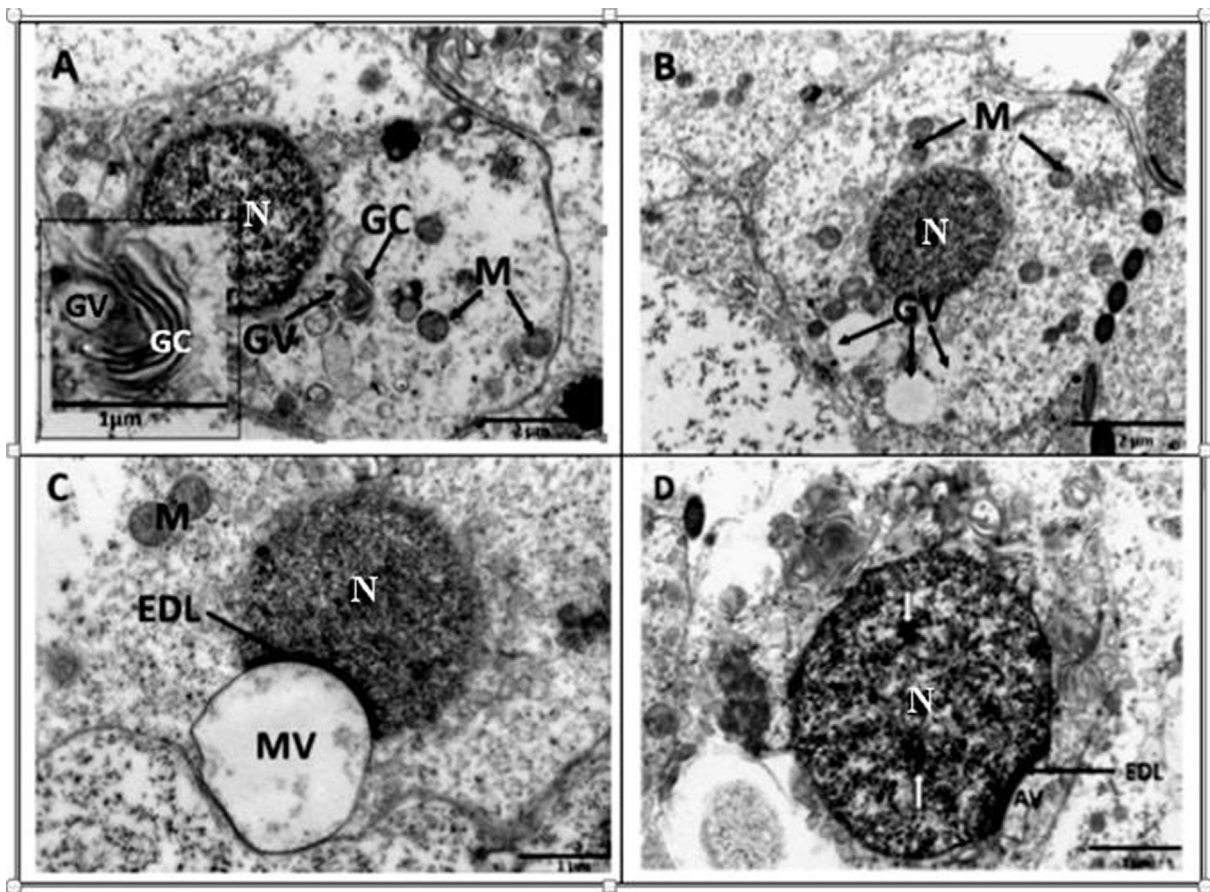


Fig. 2. Transmission electron microscope photomicrographs of round spermatids in the African sideneck turtle. A. Observe the prominent Golgi complex (GC) with budding vesicles (GV); N: nucleus; M: mitochondria. Inset: Golgi complex with budding vesicle. B. Round spermatid with conspicuous Golgi vesicles (GV) of various sizes which later coalesce to form a macrovesicle. Mitochondria (M) are evenly distributed around the nucleus (N). C. A macrovesicle (MV) formed as a result of coalescence of small vesicles attached to the nuclear membrane of a round spermatid. An electron dense layer (EDL) is formed at the point of attachment between the nucleus (N) and macrovesicle. Juxtanuclear mitochondria (M) are also present. D. Round spermatid subsequent to the flattening of the proacrosomal vesicle, resulting in the formation of the acrosomal vesicle (AV). The electron dense layer (EDL) still intact, while the nucleus (N) shows sparse areas of deep staining chromatin (white arrows).

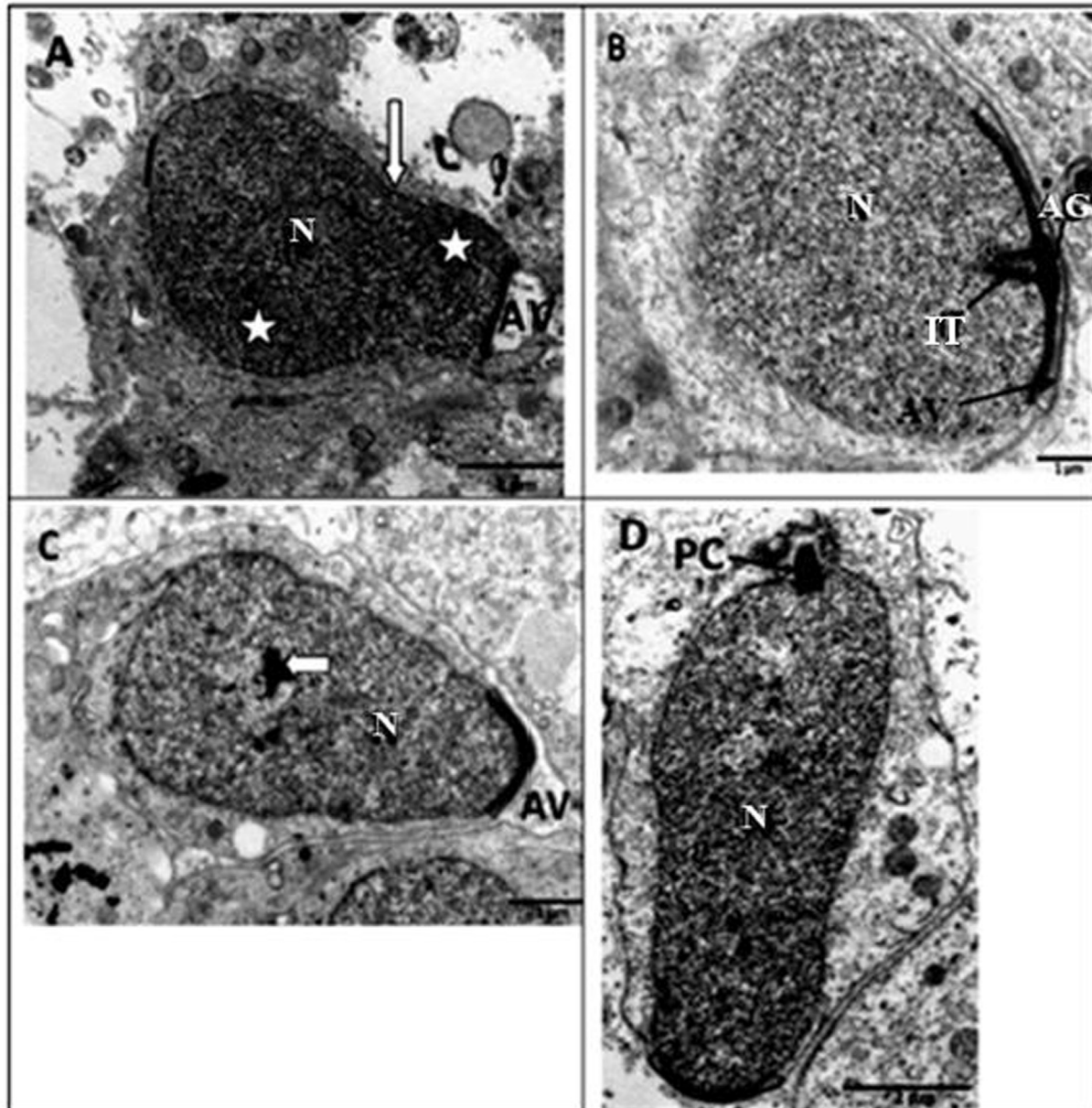


Fig. 3. Transmission electron microscope photomicrographs of late round and elongating spermatids in the African sideneck turtle. A. Late round spermatid, N: nucleus; AV: acrosomal vesicle. Note the point of nuclear elongation (white arrow) and condensation (asterisks). B. Early stage in the formation of an elongating spermatid. AG: acrosome granule; AV: Acrosomal vesicle; two parallel intranuclear tubules (IT) have formed in the interior of the nucleus (N). C. Elongating spermatid showing centrally-placed nuclear chromatin (white arrow) within the nucleus (N). Note the streamlined acrosomal vesicle (AV) assuming a pointed shape. D. Elongating spermatid with the proximal centriole (PC) at the caudal end of the nucleus (N). Note that the nuclear chromatin is distributed as a heterogenous mass.

proximal centriole is formed at the caudal region of the nucleus (Fig. 3D). In addition, the nuclear chromatin becomes distributed as a heterogenous mass (Fig. 3D).

Progressively, nuclear chromatin of the elongating spermatid condenses, the spermatid elongates and subsequently becomes surrounded by microtubules of the manchette, which are observed in both longitudinal and cross sections (Fig. 4A & B). The microtubules of the circular manchette are thicker walled than those of the longitudinal manchette (Fig. 4A & B). Subsequent to chromatin condensation, slanting manchettes surround the elongating spermatid (Fig. 4C). As nuclear elongation continues, the acrosomal vesicle develops into the acrosomal complex which is a conical, elongated, membrane-bound vesicle (Fig. 5). The acrosomal complex comprises: a sub-acrosomal cone (thin electron lucent layer underlying the acrosome); an outer cortex region and inner

medulla; nuclear tip and the nucleus basally (Fig. 5 A-E). Endonuclear tubes extend through the centre of the nucleus and appear as canals in cross-sectional views (Fig. 5C-E).

4. Discussion

The pattern of arrangement of germs cells within the seminiferous tubules of the African sideneck turtle is similar to earlier reports in other species of turtles, as well as in reptiles (Sever et al., 2002; Vieira et al., 2004, 2005; Chen et al., 2006; Vieira et al., 2007; Zhang et al., 2007; Al-Dokhi et al., 2007; Gribbins et al., 2008, 2010; Gribbins, 2011; Rheubert et al., 2010a, 2010b; Rheubert et al., 2011). The successive layers of germs within the seminiferous tubules of the African sideneck turtle are representative of the different stages of cell division (mitosis and meiosis) and

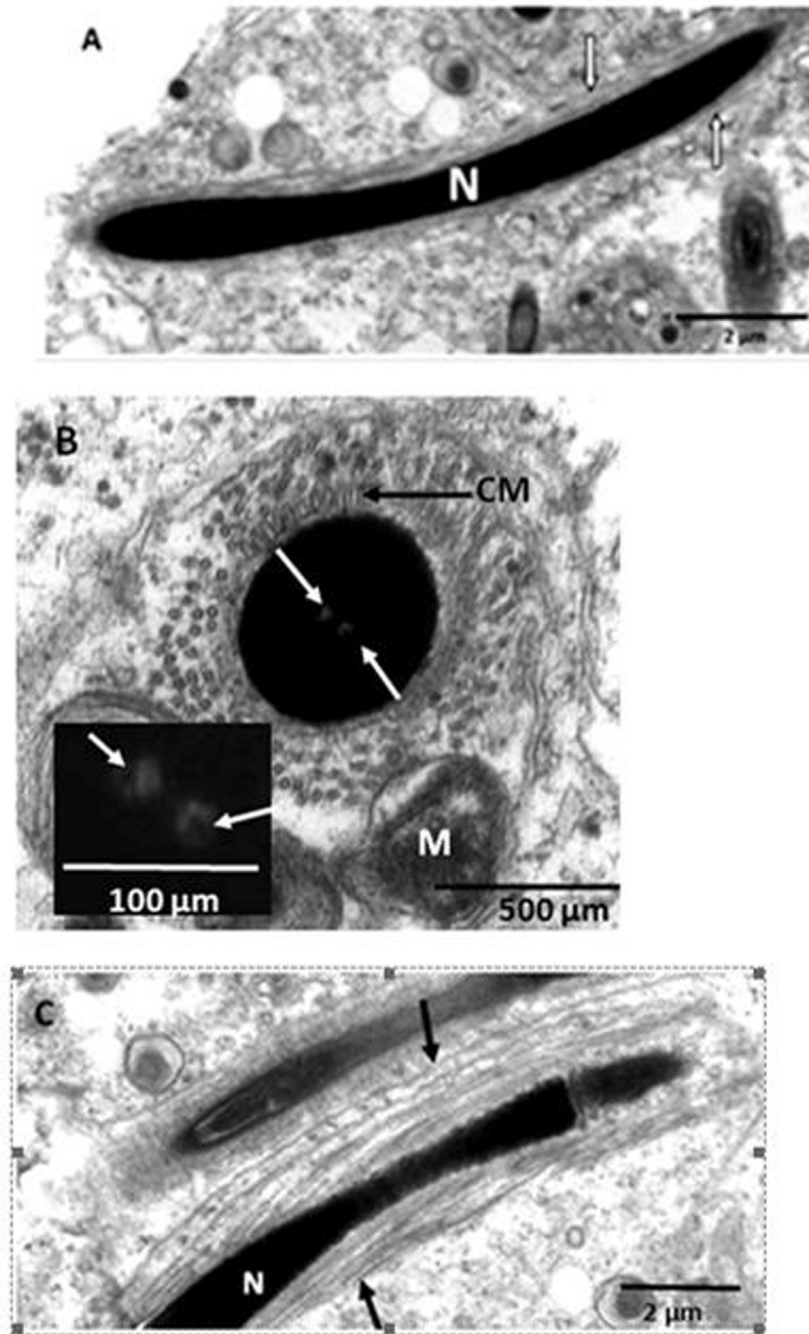


Fig. 4. Transmission electron microscope photomicrographs of elongating spermatids in the African sideneck turtle. A. Longitudinal section of an elongating spermatid. Longitudinal microtubules of the manchette (white arrows) surround the nucleus (N). B. Cross section of an elongating spermatid showing circular microtubules of the manchette (CM) surrounding the nucleus. The microtubules are partially surrounded by mitochondria while the nucleus bears endonuclear canals (white arrows). Inset: endonuclear canals (white arrows). Note that the circular microtubules of the manchette are thicker than the longitudinal type shown in Fig. 4A. C. Longitudinal section of an elongating spermatid. Slanting microtubules of the manchette (black arrows) surround the nucleus (N).

differentiation (spermiogenesis) taking place in the testicular tissue of the turtle. A major function of spermatogonia is to produce a large population of clonal germ cells that can then enter the other phases of spermatogenesis. Since large numbers of spermatozoa are typically needed for successful fertilization, the rapid and successive divisions of the spermatogonial population fulfil this requirement (Roosen-Runge, 1977).

Acrosomal vesicle morphogenesis, the initial feature of sperm head differentiation observed in the study, conforms to the general features of sperm head differentiation earlier reported in reptiles (Dehlawi and Ismail, 1990; Dehlawi et al., 1992; Al-Dokhi, 2006;

Al-Dokhi, 2009). In the African sideneck turtle, acrosome vesicle formation begins with Golgi vesicles merging at the apex of the spermatid nucleus. The close association between the Golgi complex and acrosomal vesicle alludes to the origin of the vesicles from the Golgi complex. Evidently, the pro-acrosomal vesicle is formed as a result of fusion of the smaller vesicles released from the trans-face of the Golgi complex. Therefore, acrosomal vesicle morphogenesis in the African sideneck turtle requires the Golgi complex cisternae and the associated vesicles in continuous contact with the resultant pro- and acrosomal vesicles, respectively. Thus, the development of pro- and acrosomal vesicles requires a

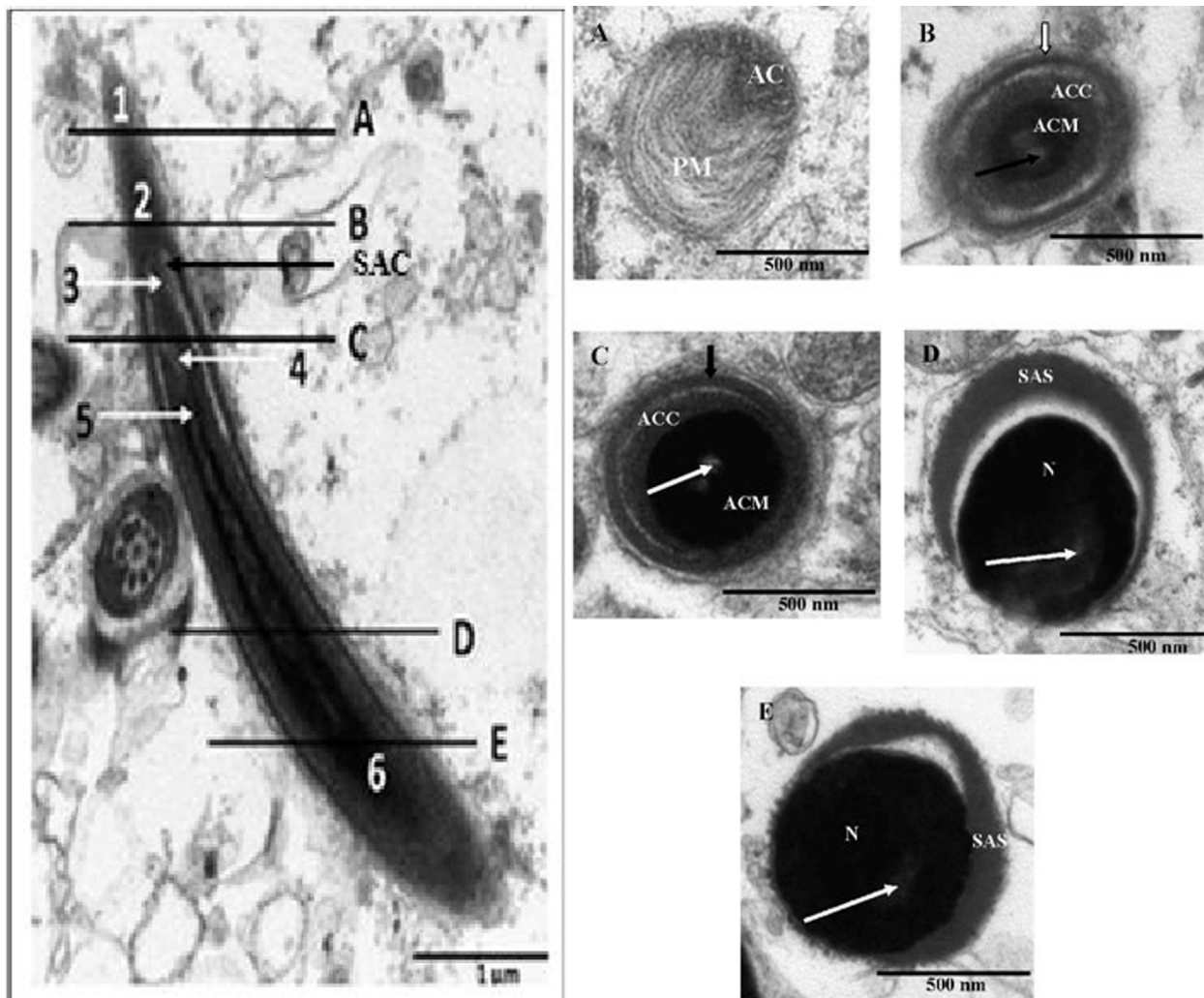


Fig. 5. Left: Transmission electron microscope photomicrographs of the longitudinal view of the acrosomal complex in the African sideneck turtle. 1: Plasma membrane of acrosome; 2: Acrosome; 3: Subacrosomal space; 4: Electron lucent endonuclear canal; 5: Nuclear tip; 6: Nucleus; SAC: Sub-acrosomal cone. Right: Cross sectional views of serial sections of the acrosome complex in the African sideneck turtle. A. Cross sectional view of the acrosomal complex sectioned at A (level of the plasma membrane just cranial to the acrosome). AC: Acrosome. PM: Plasma membrane. B. Cross sectional view of the acrosomal complex sectioned at B (level of the acrosome). ACC: Acrosome cortex. ACM: Acrosome medulla. White arrow: Acrosomal cap. Black arrow: Electron lucent endonuclear canal. C. Cross sectional view of the acrosomal complex sectioned at C (level of the subacrosome). ACC: Acrosome cortex. ACM: Acrosome medulla. Black arrow: Acrosomal cap. White arrow: Electron lucent endonuclear canal. D. Cross sectional view of the acrosomal complex sectioned at D (mid level of nucleus). SAS: Subacrosomal space. N: Nucleus. White arrow: Electron lucent endonuclear canal. E. Cross sectional view of the acrosomal complex sectioned at E (level of the base of nucleus). SAS: Subacrosomal space. N: Nucleus. White arrow: Electron lucent endonuclear space.

continuous supply of the substances released from the Golgi complex. These findings concur with previous reports on reptilian acrosomal vesicle morphogenesis (Vieira et al., 2007; Zhang et al., 2007; Al-Dokhi, 2009; Rheubert et al., 2016). The close association between the Golgi complex and acrosomal vesicle has been described for sphenodon (Healy and Jamieson, 1994), squamates (Gribbins et al., 2009) and other archosaurs, including birds (Aire, 2007) and crocodiles (Wang et al., 2008; Gribbins et al., 2010). However, in the green iguana (*Iguana iguana*) rough endoplasmic reticulum is in close association with the Golgi complex (Ferreira and Dolder, 2002).

The single acrosomal granule observed in the African sideneck turtle is similar to those reported in the freshwater turtle, *Maurymys caspica* (Al-Dokhi and Al-Wasel, 2001a), soft shell turtle *Pelodiscus sinensis* (Zhang et al., 2007), American alligator, *Alligator mississippiensis* (Gribbins et al., 2010), Mediterranean gecko, *Hemidactylus turcicus* (Rheubert et al., 2011) and Eastern French lizard, *Sceloporus undulatus* (Rheubert et al., 2016). However, two acrosomal granules have been reported in the five-lined skink, *Mabuya quinquetaeniata* (Ismail, 1997). As observed in the present study,

the acrosomal granule develops after the attachment of the acrosomal vesicle to the nucleus of the spermatid. This is similar to observations made in other reptiles, including the house gecko (*Ptyodactylus hasselquisti*) and the lizards *Agama adramitana*, as well as *Acathodactylus boskinus* (Dehlawi and Ismail, 1990; Al-Dokhi, 2006, 2009). Interestingly, the lizard *Stenodactylus selvini* manifests the acrosomal granule before the attachment of the acrosomal vesicle to the spermatid nucleus (Dehlawi and Ismail, 1990; Al-Dokhi, 2009; Rheubert et al., 2016).

Sperm nuclear morphogenesis, comprising elongation and chromatin condensation has been described as the most important event of spermiogenesis (Zhang et al., 2007). The pattern of nuclear elongation, as well as the sparse distribution of deep staining nuclear chromatin in the elongating spermatid of the African sideneck turtle is similar to those of the soft shell turtle *Pelodiscus sinensis* (Zhang et al., 2007). However, only one endonuclear canal was reported in the elongating spermatid of the soft shell turtle *Pelodiscus sinensis* (Zhang et al., 2007), in contrast, two were observed in the African sideneck turtle. The uniformly diffuse nuclear chromatin and progressive nuclear condensation pattern

seen in this study is typical of chelonians (Healy and Jamieson, 1994; Al-Dokhi and Al-Wasel, 2001b; Zhang et al., 2007).

The microtubules of the manchette have been implicated in the nuclear elongation stage of spermiogenesis and are considered a commonly observed structure during this phase in reptiles (Russell et al., 1990; Ferreira and Dolder 2002; Gribbins et al., 2010). It is not known whether or not both longitudinal and circular microtubules of the manchette are needed for nuclear elongation in turtles as some squamates have been reported to have only longitudinal microtubules in their spermatids (Dehlawi et al., 1992; Gribbins et al., 2010). Zhang et al. (2007) speculated that the manchette may apply a mechanical force against the sperm nucleus. This force results in further nuclear condensation of the elongating spermatid, allowing for a major reduction in nuclear volume. The streamlining of the spermatid is thought to assist in the preservation of the eventual spermatozoa, protecting it from physical damage or mutation during storage and transportation (Browder, 1984). In lizard, *Tropidurus itambere*, the manchette has been reported to initially wrap helically around the nucleus, and then straightens into a longitudinal arrangement as nuclear condensation continues (Hofling, 1978). Interestingly, microtubules have not been observed in the spermatids of lizard species, such as, *Dinnodon rufozonatum* (Cai et al., 1997), *Natrix piscator* (Gao et al., 2001) and *Takydromus septemtrionalis* (Liu et al., 2005).

The longitudinal and circular microtubules of the manchette, observed in the late spermatid, have also been reported in other species of turtle, as well as in reptiles (Rheubert et al., 2011; Zhang et al., 2007). However, contrary to the observations made in the present study, the microtubules of the longitudinal manchette of the soft shell turtle (*Pelodiscus sinensis*) are thicker than those of the circular component (Zhang et al., 2007). However, this is different from the *Caiman crocodylus* (Saita and Comazzi, 1987) in which the microtubules of the longitudinal manchette are thicker walled than those found in the circular manchette (Gribbins et al., 2010).

The slanting manchette that surrounds the nucleus of the elongating spermatid in the African sideneck turtle is similar to that reported in the freshwater turtle, *Maurymes caspica* (Al-Dokhi and Al-Wasel, 2001a), as well as in the soft shell turtle, *Pelodiscus sinensis* (Zhang et al., 2007). However, a slanting manchette is absent in the eastern French lizard, *Sceloporus undulatus* (Rheubert et al., 2016). Previous authors have suggested that in reptiles the manchette (circular longitudinal or slanting), plays an important role in nuclear shaping and organelle movement during spermiogenesis (Dehlawi et al., 1992; Al-Dokhi, 2006; Zhang et al., 2007).

Acrosomal vesicle morphogenesis in the African sideneck turtle results in a highly compartmentalized acrosome divisible into a cortex and medulla. This finding is consistent among reptilian models (Gribbins and Rheubert, 2014). The highly compartmentalized reptilian acrosome may be indicative of the presence of a unique physiological degradation mechanism of the cumulus granulosa cells, zona pellucida, and oocyte membrane during the sperm-egg interaction (Rheubert et al., 2016). This process of degradation involves hydrolytic enzymes, principally hyaluronidase, which the sperm acrosomal cap contains (Al-Dokhi, 2009). It is thought that enzymes responsible for degrading the cumulus granulosa cells in reptiles are located within the acrosomal cortex and medulla (Rheubert et al., 2016). The enzymes are released upon membrane fusion during fertilization (Rheubert et al., 2016).

It can be concluded that acrosome vesicle development and spermatid nuclear morphogenesis vary among reptiles and turtles specifically, though the processes involved are basically similar. The observed developmental variations are expected to be valuable in future phylogenetic studies and potentially serve to test certain

hypotheses concerning the reproductive status of turtle species. Information made available by this study will add to the growing database of spermatid morphology in turtles, thereby providing insights into variations in mature sperm morphology in the species.

Conflict of interest

The authors have no conflict of interest to declare.

Acknowledgements

The authors are grateful to the University of Ibadan, Nigeria for Senate Research Grants (SRG/FVM/2010/4A and SRG/FVM/2010/1B) that aided this study. Dr S.G. Olukole is a Postdoctoral Fellow, Department of Anatomy and Physiology, Faculty of Veterinary Science, University of Pretoria, South Africa.

References

- Aire, T.A., 2007. Anatomy of the testis and male reproductive tract. In: Jamieson, B. G.M. (Ed.), *Reproductive biology and phylogeny of birds*. Science Publishers, Enfield, NH, pp. 37–113.
- Al-Dokhi, O.A., 2004. Electron microscopic study of Sperm head differentiation in the Arabian horned viper *Cerastes cerastes* (Squamata, Reptilia). *J. Biol. Sc.* 4 (2), 111–116.
- Al-Dokhi, O.A., 2006. Ultrastructure of sperm head differentiation in the lizard *Achatodactylus boskinus* (Squamata Reptilia). *Int. J. Zool. Res.* 2, 60–72.
- Al-Dokhi, O.A., 2009. Morphogenesis of the acrosomal vesicle during spermiogenesis in the House Gecko *Ptyodactylus hasselquisti* (Squamata Reptilia). *Int. J. Zool. Res.* 5, 360–376.
- Al-Dokhi, O.A., Al-Wasel, S., 2001a. Ultrastructure of spermiogenesis in the freshwater turtle *Maurymes caspica* (Chelonia, Reptilia). I. The acrosomal vesicle and the endonuclear canals formation. *J. Egypt Ger. Soc. Zool.* 36 (B), 93–106.
- Al-Dokhi, O.A., Al-Wasel, S., 2001b. Ultrastructure of spermiogenesis in the freshwater turtle *Maurymes caspica* (Chelonia, Reptilia). II. The nucleus elongation and chromatin condensation. *J. Union Arab. Biol. Zool.* 15 (A), 355–366.
- Al-Dokhi, O.A., Al-Wasel, S., Mubarak, M., 2007. Ultrastructure of the spermatozoa of the freshwater turtle *Maurymes caspica* (Chelonia, reptilian). *Int. J. Zool. Res.* 3 (2), 53–64.
- Al-Dokhi, O.A., Mukhtar, A., Al-Dosary, A., Al-Sadoon, M.K., 2015. Ultrastructural differentiation of sperm tail region in *Diplometopon zarudnyi* (an amphisbaenian reptile). *Saudi J. Bio. Sc.* 22, 448–452.
- Browder, L.W., 1984. *Developmental Biology*. Saunders College Publishing, New York.
- Cai, Y.F., Tang, J.Y., Pan, H.C., 1997. Electron microscopic study of sperm head formation in *Dinnodon rufozonatum*. *Acta. Anat. Sin.* 28, 94–97.
- Chen, Q.S., Zhang, L., Han, X.K., Chen, X.W., 2006. Ultrastructure of spermatozoon in soft-shelled turtle, *Trionyx sinensis*. *Acta. Zool. Sin.* 52, 415–423.
- Dehlawi, G.Y., Ismail, M.F., 1990. Studies on ultrastructure of the spermiogenesis of Saudian reptiles. 1. The sperm head differentiation in *Uromastix philbyi*. *Proc. Zool. Soci. Egypt* 21, 75–85.
- Dehlawi, G.Y., Ismail, M.F., Hamdi, S.A., Jamjoom, M.B., 1992. Ultrastructure of spermiogenesis of a Saudian reptile. The sperm head differentiation in *Agama adramitana*. *Arch. Androl* 28, 223–234.
- Ferreira, A., Dolder, H., 2002. Ultrastructural analysis of spermiogenesis in *Iguana iguana* (Reptilia: Sauria: Iguanidae). *Eur. J. Morphol.* 40, 89–99.
- Gao, J.M., Zheng, C.F., Zhang, Y.D., Zhang, Q.J., Lin, W., 2001. Seasonal changes in ultrastructure of seminiferous epithelia of the snake *Natrix piscator*. *Acta. Anat. Sin.* 32, 76–79.
- Gribbins, K.M., 2011. Reptilian spermatogenesis: A histological and ultrastructural perspective. *Spermatogenesis* 1 (3), 250–269.
- Gribbins, K.M., Rheubert, J.L., 2014. The architecture of the testis, spermatogenesis, and mature spermatozoa. In: Rheubert, J.L., Siegel, D.S., Trauth, S.E. (Eds.), *Reproductive Biology and Phylogeny of Lizards and Tuatara*. CRC Press, BocaRaton, FL, pp. 340–424.
- Gribbins, K.M., Rheubert, J.L., Collier, M.H., Siegel, D.S., Sever, D.M., 2008. Histological analysis of spermatogenesis and the germ cell development strategy within the testis of the male Western Cottonmouth Snake, *Agkistrodon piscivorus leucostoma*. *Ann. Anat.* 190, 461–476.
- Gribbins, K.M., Rheubert, J.L., Poldemann, E.H., Collier, M.H., Wilson, B., Wolf, K., 2009. Continuous spermatogenesis and the germ cell development strategy within the testis of the Jamaican Gray Anole, *Anolis lineatopus*. *Theriogenology* 72, 54–61.
- Gribbins, K.M., Siegel, D.S., Anzalone, M.L., Jackson, D.P., Venable, K.J., Rheubert, J.L., Elsey, R.M., 2010. Ultrastructure of spermiogenesis in the American Alligator,

- Alligator mississippiensis* (Reptilia, Crocodylia, Alligatoridae). J. Morphol. 271, 120–1271.
- Healy, J.M., Jamieson, B.G.M., 1994. The ultrastructure of spermatogenesis and epididymal spermatozoa of the tuatara, *Sphenodon punctatus* (Sphenodontidae, Amniota) Philo. Trans. Royal Soc. Lon. Biol. Sci. 344, 187–199.
- Hofling, M.A.C., 1978. The fine structure of nuclei during spermiogenesis in lizard *Tropidurus*. Cytologia 43, 61–68.
- Ismail, M.F., 1997. Unusual features of the sperm head differentiation in Mabuya quinquetaeniata. Arch. Androl. 39, 19–23.
- Kirkpatrick, D.T., 1995. An Essay on Taxonomy and the Genus *Pelusios*. Available at: <http://www.unc.edu/~dtkirkpa/stuff/pel.html>, (accessed 22.02.13).
- Liu, Y.Z., Zhang, Y.P., Fang, Z.X., 2005. Ultrastructural studies on spermiogenesis of *Takydromus septentrionalis*. Acta. Anat. Sinica. 36, 436–441.
- Olukole, S.G., Aina, O.O., Okusanya, B.O., 2010. Morphometric analysis of the external body anatomy of the African sideneck turtle. Proceedings of the 30th Annual symposium of the International Sea Turtle Biology and Conservation Society, p. 256.
- Olukole, S.G., Okusanya, B.O., Oyeyemi, M.O., Oke, B.O., 2013. Sperm morphological characteristics and morphometry in the African sideneck turtle (*Pelusios castaneus*). Asian J. Exp. Biol. Sci. 4 (4), 607–612.
- Olukole, S.G., Oyeyemi, M.O., Oke, B.O., 2014. Spermatogenic cycle of the African sideneck turtle *Pelusios castaneus* (Schweigger, 1812) (Reptilia: Testudines). Ital. J. Zoo. 81 (1), 25–31.
- Rao, R.J., Shaad, F.U., 1985. Sexual cycle of the male freshwater turtle. *Trionyx gangeticus* (Cuvier) Herpetologica 41 (4), 433–437.
- Rheubert, J.L., Wilson, B.S., Wolf, K.W., Gribbins, K.M., 2010a. Ultrastructural study of spermiogenesis in the Jamaican Gray Anole, *Anolis lineatopus* (Reptilia: Polychrotidae). Acta. Zool. (Stockholm) 91, 484–494.
- Rheubert, J.L., McMahan, C.D., Sever, D.M., Bundy, M.R., Siegel, D.S., Gribbins, K.M., 2010b. Ultrastructure of the reproductive system of the Black Swamp Snake (*Seminatrix pygaea*). VII. Spermatozoon morphology and evolutionary trends of sperm characters in snakes. J. Syst. Zool. Evol. Res. 48, 366–375.
- Rheubert, J.L., Siegel, D.S., Venable, K.J., Sever, D.M., Gribbins, K.M., 2011. Ultrastructural description of spermiogenesis within the Mediterranean Gecko, *Hemidactylus turcicus* (Squamata: Gekkonidae). Micron 42, 680–690.
- Rheubert, J.L., Sever, D.M., Siegel, D.S., Gribbins, K.M., 2016. Ultrastructural analysis of spermiogenesis in the Eastern Fence Lizard, *Sceloporus undulatus* (Squamata: Phrynosomatidae). Micron 81, 16–22.
- Rosen-Runge, E.C., 1977. The Process of Spermatogenesis in Animals. Cambridge University Press, England.
- Russell, L.D., Hikim, S.A.P., Ettlin, R.A., Clegg, E.D., 1990. Histological and histopathological evaluation of the testis. Cache River Press, Clearwater FL.
- Saita, A., Comazzi, M., 1987. Electron microscope study of spermiogenesis in *Caiman crocodylus*. Boll. Zool. 4, 307–318.
- Sever, D.M., Ryan, T.J., Stephens, R., Hamlett, W.C., 2002. Ultrastructure of the reproductive system of the black swamp snake (*Seminatrix pygaea*). III. Sexual segment of the male kidney. J. Morphol. 252, 238–254.
- Teixeira, R.D., Vieira, G.H.C., Colli, G.R., Bao, S.N., 1999. Ultrastructural study of spermatozoa of the neotropical lizards, *Tropidurus semitaeniatus* and *Tropidurus torquatus* (Squamata, Tropiduridae). Tissue & Cell 31 (3), 308–317.
- Vieira, G.H.C., Colli, G.R., Bao, S.N., 2004. The ultrastructure of the spermatozoon of the lizard *Iguana iguana* (Reptilia, Squamata Iguanidae) and the variability of sperm morphology among iguanian lizards. J. Anat. 204, 451–464.
- Vieira, G.H.C., Colli, G.R., Bao, S.N., 2005. Phylogenetic relationships of corytophanid lizards (*Iguana*, Squamata, Reptilia) based on partitioned and total evidence analyses of sperm morphology, gross morphology, and DNA data. Zoo. Scripta. 34, 605–625.
- Vieira, G.H.C., Cunha, L.D., Scheltinga, D.M., Glaw, F., Colli, G.R., Bao, S.N., 2007. Sperm ultrastructure of hoplocercid and oplurid lizards (*Sauropsida*, Squamata, *Iguana*) and the phylogeny of Iguania. J. Zool. Syst. Evol. Res. 10, 439–469.
- Wang, L., Wu, X., Xu, D., Wang, R., Wang, C., 2008. Development of testis and spermatogenesis in *Alligator sinensis*. J. Appl. Anim. Res. 34, 23–28.
- Zhang, L., Xiang-Kun, H., Mei-Ying, L., Hui-Jun, B., Qiu-Sheng, C., 2007. Spermiogenesis in the Soft-Shell Turtle, *Pelodiscus sinensis*. Anat. Rec. 290, 1213–1222.